Yaw moment Lyapunov based control for In-Wheel-Motor-Drive Electric Vehicle

Hind Laghmara, Moustapha Doumiati, Reine Talj, Ali Charara

Yaw moment Lyapunov based control for In-Wheel-Motor-Drive Electric Vehicle ⋆

H. Laghmara * **M. Doumiati** ** **R. Talj** * **A. Charara** *

* *Sorbonne Universités, Université de Technologie de Compiègne, CNRS, Heudiasyc, UMR 7253, 57 avenue de Landshut, CS 60319, 60203 Compiègne cedex, France (reine.talj@hds.utc.fr)*
** *ESEO-Angers, High School of Engineering, 10 Bd Jean Jeanneteau, 49100 Angers, France (moustapha.doumiati@eseo.fr)*

Abstract: The new generation of electric vehicles, also called in-wheel-motor-drive electric vehicles (IWM-EVs), will replace the traditional power-train by on-hub motors. Consequently, it will offer new options and flexibilities in motion control due to its structural merits, i.e the longitudinal force of each wheel could be controlled independently. This paper proposes an advanced direct yaw moment control strategy to improve IWM-EV steerability and stability. The proposed integrated control involves two coordinated standalone Lyapunov model-based controllers. Coordination is ensured according to the vehicle dynamic states evolution in the phase plane defined by the body sideslip angle and its rate. The control objective in the linear driving zone is to enhance the vehicle steering response by tracking a certain reference yaw rate. However, when the vehicle reaches the handling limits, the primary objective becomes to stabilize the vehicle while reducing a vehicle stability index. The yaw moment generated to provide control goals is then converted into four torque inputs of the four in-wheel motors. An algorithm is proposed for an effective torques distribution to maintain vehicle longitudinal velocity. Simulation results carried out on a full nonlinear IWM-EV model confirm the ability of the developed control scheme to improve vehicle handling and directional stability.

Keywords: Vehicle dynamics; In-wheel-motor-drive electric vehicle; Integrated control; Lyapunov direct method.

1. INTRODUCTION

1.1 Motivation

In view of the expansion of eco-friendly systems, the combustion engines are being replaced by less polluting electric motors. Nowadays, boosted by the dramatic improvement and development of electric motors, batteries, and high control technologies, Electric Vehicles (EVs) are seeing a great increase in the market. From the viewpoint of vehicle dynamics, it is possible to install small and powerful electric motors directly connected to two or four wheels to drive the vehicle [Chen et al. (2013); Doumiati et al. (2014)]. This category of EVs is called In-Wheel-Motor-Drive EVs (IWM-EVs), where each motor can be controlled independently for both braking and driving purposes. Compared to internal combustion engine, the time response of an electric motor is much better, and the output torque of the motor is easier to measure by using the electric motor current [Shino et al. (2001)]. Consequently, it is possible to realize a more accurate motion control to an EV actuated by in-wheel motors.
Vehicle driving safety and comfort remains an actual and a timeless problem. Road vehicle is considered as a very complex system composed of various subsystems which interact with each other. Consequently, variables describing the vehicle dynamics are highly coupled, and are complicated to control. This paper focuses on the lateral motion control of a four IWM-EV with no steer-by-wire.
Over the past few years, a great deal of research on integrated motion control has been developed. The basic purpose of the lateral motion control systems is to assist the vehicle handling to be close to a linear vehicle handling characteristics familiar to the driver. The vehicle lateral dynamics must be bounded in a stable handling region to avoid drifting or spinning situations. Because the yaw motion of the vehicle is determined by the yaw moment, the vehicle lateral motion can be achieved by controlling the driving and braking torques of the in-wheel motors [Zhai et al. (2016)]. Mainly two design topologies, bottom-up and top-down, draw the attention of researchers on integrated control design [Doumiati et al. (2013)]. The bottom-up multi-layer control approach is formulated by adding a level of supervision to different subsystem controllers to deal with their interactions; i.e, authors in [Zhao et al. (2015); Zhai et al. (2016)] develop multi-layer controllers based on sliding-mode theory to improve the vehicle motion. On the other side, the top-down centralized structure is established using a unified global multivariable controller to make all control decisions, and to distribute the generic actuation to corresponding actuators; i.e, authors in [Doumiati et al. (2013); Doumiati et al. (2014); Gaspar et al. (2015)] propose centralized controllers according to $\mathcal{H}_\infty$ control theory extended to linear parameter varying systems to enhance global chassis control. The multi-layer control approach is adopted in this paper in order to formulate a simple and reliable direct yaw moment control scheme convenient for real-time implementation.

⋆ This work was carried out and funded in the framework of the Labex MS2T. It was supported by the French Government, through the program "Investments for the future" managed by the National Agency for Research (Reference ANR-11-IDEX-0004-02). This work was also carried out in the framework of the French "Hauts-de-France" region project SYSCOVI. SYSCOVI is jointly financed by the European Union. Europe engages in Picardie with the European Fund of Regional Development FEDER.

1.2 Contributions

The aim of the proposed control structure in this paper is twofold: enhancing vehicle steerability and stability. The proposed method improves the IWM-EV yaw motion by directly acting on in-wheel-motors and distributing differential longitudinal forces (driving, braking, or both) between inner and outer wheels according to the vehicle running status. From the viewpoint of vehicle dynamics, the yaw rate and sideslip motions are deeply concerned with vehicle stability and handling control. Most of the methods found in literature seek to monitor the stability of the vehicle by reducing the slip angle [Shino et al. (2001); Nam et al. (2012); Chen et al. (2013); Shuai et al. (2013); Zhai et al. (2016)]. This paper suggests a novel approach that handles the stability problem by regulating a dynamic stability index evaluated in the phase plane (sideslip angle and its rate). On the other hand, steerability is controlled by acting on the EV yaw rate.
Vehicle dynamics analysis proves that a good steerability leads to instability, and vice-versa [Crolla et al. (2004); Doumiati et al. (2014)]. The conflicts in control objectives especially appear at the handling limits as the major two variables characterizing the lateral vehicle dynamics behavior become strongly coupled, and the required moments controlling the two variables may be opposite. The control approach proposed in the following involves two controllers coordinated in a manner to avoid conflicts between stability and steerability objectives. One controller cares for steerability, while the second one monitors stability. The two controllers are developed independently, and control laws are formulated according to Lyapunov direct method theory [Haddad et al. (2008)]. Lyapunov approach is chosen to warranty stability, robustness, and sufficient fast convergence to track the desired dynamics behavior. The yaw moment generated by steerability and stability controllers is then transformed to wheel torque signals according to a torque allocation algorithm aiming to minimize the influence on longitudinal vehicle velocity.

This paper consists of several sections. Section 2 analyzes the control tasks, and defines stability and steerability control modes. Section 3 deals with the global control architecture, and develops the stability and steerability controllers. Numerical simulations are performed and analyzed in Section 4 through a platform developed in Matlab/Simulink environment. Conclusions and discussions are given in Section 5.

2. CONTROL TASKS AND JUDGMENT OF CONTROL MODES

For a pertinent coordination avoiding conflicts between stability and steerability objectives, it is fundamental to start analyzing some vehicle dynamics behavior.

2.1 Coordination between steerability and stability control

Vehicle dynamics analysis shows that the vehicle's yaw rate and sideslip angle are highly coupled variables. To improve vehicle steering response (called steerability, also known as maneuverability), yaw motion could be accelerated and consequently the sideslip motion of the vehicle. On the contrary, for stability reason, the sideslip motion must be bounded and thus the yaw motion of the vehicle to avoid critical situations. Interference between steerability and stability becomes critical when the vehicle approaches the handling limits inducing conflicts in control objectives [Crolla et al. (2004); Doumiati et al. (2014)]. To face such situations, the proposed yaw moment control formulates the following:

- The objective of steerability has the priority when the vehicle moves in a reference stability region (normal driving situations). Stability is not in question in this zone, and thus, only steerability control mode is activated.
- When the side slip angle becomes large, stability dominates the objective at the limits of handling. Steerability is not the primary concern in this region, and therefore, only stability control mode is activated.

To judge the control mode operation which is stability or steerability, the vehicle operating zone must be identified.

2.2 Vehicle operating zone

The vehicle operating point ranges from normal driving to handling limits. Different existing studies propose some metrics to distinguish between stable and unstable driving zones. As example, yaw rate error constraints, *yaw rate-sideslip angle* phase plane, and *sideslip angle - sideslip angle rate* phase plane methods were used in literature to judge the driving zone [Zhai et al. (2016)]. This study adopts the *sideslip angle - sideslip angle rate* phase plane method due to its reliability and effectiveness. The stability index is defined as [Doumiati et al. (2013); Zhai et al. (2016)]:

$$\lambda = B_1\dot{\beta} + B_2\beta, \tag{1}$$

where B_1 and B_2 are experimental boundary parameters mainly function of the road friction μ. The stability region ensuring a safe driving envelope is defined for:

$$|\lambda| < 1. \tag{2}$$

This means that the vehicle falls into the unstable region only when the sideslip angle becomes large and has the same sign as its derivative.

3. CONTROL SCHEME DESIGN

The structure of the proposed control system is model-matching controller which makes the vehicle follows a desired dynamic model by regulating stability index and yaw rate variables. As seen in Figure 1, the proposed yaw motion controller responds to the yaw rate and the stability index errors, $e_{\dot{\psi}}$ and e_λ, respectively. The controller outputs are the four wheels braking/traction torques needed to adjust the vehicle dynamics behavior. According to the coordination strategy discussed in Section 2, and as explained later, the controller focuses on one input variable at a time according to the vehicle driving operating zone. It is supposed that the required measurement signals to make control decisions (notably $\dot{\psi}$, β, and $\dot{\beta}$), are available through hard or soft sensors [Doumiati et al. (2012)].
Referring to Figure 1, the proposed yaw moment controller is hierarchical and designed in 2 layers:

a) The upper controller provides the corrective yaw moment, M_z, needed to make the yaw rate and stability index trace their desired values. It includes the stability and steerability coordinated standalone controllers, and the vehicle dynamics supervisor that judges the control mode according to the recognition of the vehicle driving status.
b) The lower controller converts the stabilizing yaw moment generated by the upper controller into effective braking/driving torques generated by the electric motors. A torque allocation method is proposed to counteract the undesired yaw motion. The generated wheel torques are transformed as interactions between tires and ground to maintain stability.

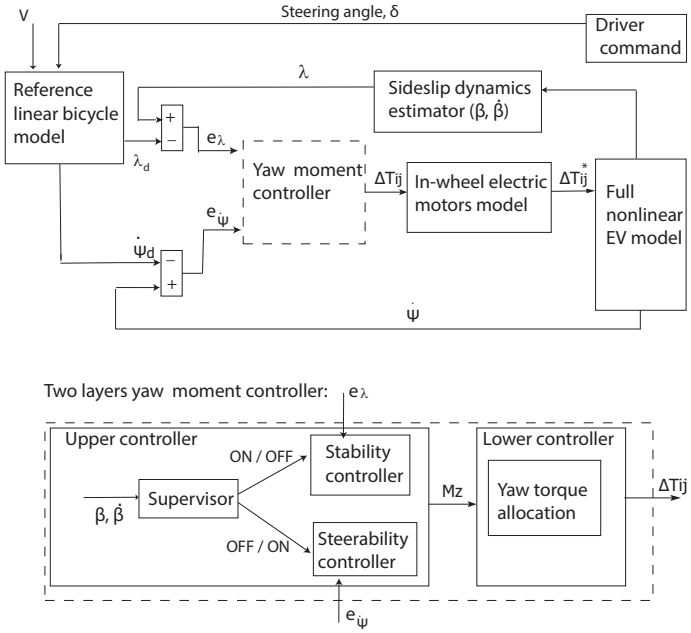

Fig. 1. Global control scheme.

3.1 Reference model

The reference signals generator is based on a simplified 2-DOF (Degree Of Freedom) planar linear bicycle model as shown in Figure 2. It provides the desired values to be followed by the controllers, notably the yaw rate $\dot{\psi}_d$, the side slip angle β_d and its rate $\dot{\beta}_d$. These values are mainly function of the driver's steering angle δ, the vehicle's longitudinal velocity V_x, and the road friction μ. The developed model assumes small side slip angle, and neglects nonlinear dynamics. Roll, pitch, and longitudinal behaviors are also simplified. Therefore, equations governing the lateral and yaw motions can be expressed as [Rajamani et al. (2012); Doumiati et al. (2013)]:

- Equation of lateral motion:

$$mv\left(\dot{\beta}-\dot{\psi}\right)=C_f\left(\delta-\beta-l_f\frac{\dot{\psi}}{V_x}\right)+C_r\left(-\beta+l_r\frac{\dot{\psi}}{V_x}\right) \tag{3}$$

- Equation of yaw motion:

$$I_z\ddot{\psi}=C_f\left(-l_f\frac{\dot{\psi}}{V_x}-\beta-\delta\right)l_f+C_r\left(\beta-l_r\frac{\dot{\psi}}{V_x}\right)l_r \tag{4}$$

where m is the vehicle's mass, $l_{f,r}$ are the distances from the vehicle center of gravity to the front and rear axles, I_z is the vehicle's yaw inertia, β is body sideslip angle, and $C_{f,r}$ are the cornering stiffness per front and rear axles, respectively. For a safe drive, these references must be saturated by the physical limits imposed by μ, to ensure that the slip angle does not become too large during the vehicle's trajectory. Referring to [Rajamani et al. (2012)], the limitation constraints are:

$$\dot{\psi}_{max}|\leq\left|\frac{0.85\mu g}{V_x}\right|\ \&\beta_{max}=\arctan(0.02\mu g), \tag{5}$$

where g is the gravitational acceleration.

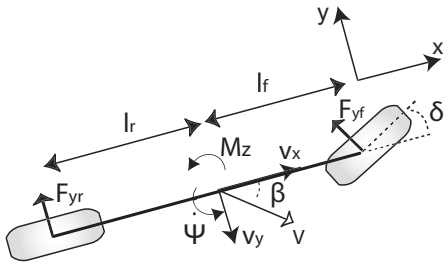

Fig. 2. 2-DOF model of the lateral vehicle dynamics.

3.2 Synthesis vehicle model

In the following subsections, the vehicle model used for the linear control laws design is based on the reference linear model described in the previous section while adding a direct yaw moment M_z as a control input variable. The state-space representation of the vehicle is therefore expressed as:

$$\begin{bmatrix}\dot{\beta}\\ \ddot{\psi}\end{bmatrix}=\begin{bmatrix}a_{11} & a_{12}\\ a_{21} & a_{22}\end{bmatrix}\begin{bmatrix}\beta\\ \dot{\psi}\end{bmatrix}+\begin{bmatrix}b_1\\ b_2\end{bmatrix}\delta+\begin{bmatrix}0\\ b_3\end{bmatrix}M_z, \tag{6}$$

where: $a_{11}=\frac{-C_f-C_r}{mV_x}$, $a_{12}=-1+\frac{-C_fl_f+C_rl_r}{mV_x^2}$, $a_{21}=\frac{-C_fl_f+C_rl_r}{I_z}$, $a_{22}=\frac{-C_fl_f^2-C_rl_r^2}{I_zV_x}$, $b_1=\frac{C_f}{mV_x}$, $b_2=\frac{C_fl_f}{I_z}$, $b_3=\frac{1}{I_z}$.

3.3 Stability control

The stability controller is mainly used for emergency maneuvers, and is disabled in normal driving situations. An excessive body sideslip angle makes the vehicle's yaw motion insensitive to the driver's steering input due to the nonlinear tire characteristics. Such cases lead to instability and critical/dangerous driving situations. When the vehicle goes beyond the stable region defined in (2), the stability controller should generate a stabilizing yaw moment to bound the body sideslip dynamics, and maintain lateral stability. In literature, most researchers often only control the side slip angle to impose stability. In the present paper, it is proposed to reach stability by reducing the stability index tracking error $e_\lambda=\lambda-\lambda_d$. The control law proposed in the following is based on Lyapunov direct method providing robustness and closed-loop system stability [Haddad et al. (2008)].

Let V_1 be the candidate Lyapunov function for stability control:

$$V_1=\frac{1}{2}e_\lambda^2, V_1>0, V_1(0)=0. \tag{7}$$

V_1 is an energy function depending on the stability index tracking error. To ensure that $e_\lambda\to 0$ as $t\to+\infty$, V_1 must be a Lyapunov function with $\frac{dV_1}{dt}=\dot{V}_1<0, \forall\ e_\lambda\neq 0$. The exponential stability with a decay rate k_1 could be verified if:

$$\dot{V}_1=-k_1V_1=-\frac{k_1}{2}e_\lambda^2, \forall k_1>0. \tag{8}$$

According to (1), desired and actual stability indexes, λ_d and λ, respectively, are given by:

$$\lambda=B_1\dot{\beta}+B_2\beta \tag{9}$$

$$\lambda_d=B_1\dot{\beta}_d+B_2\beta_d. \tag{10}$$

From the simplified model representation in (6), β and β_d can be deduced:

$$\dot{\beta} = a_{11}\beta + a_{12}\dot{\psi} + b_1\delta \tag{11}$$

$$\dot{\beta}_d = a_{11}\beta_d + a_{12}\dot{\psi}_d + b_1\delta. \tag{12}$$

Therefore, by substituting (11) and (12) in (1) and (10):

$$\lambda = \alpha_1\beta + \alpha_2\dot{\psi} + +\alpha_3\delta \tag{13}$$

$$\lambda_d = \alpha_1\beta_d + \alpha_2\dot{\psi}_d + \alpha_3\delta, \tag{14}$$

where :

$$\begin{cases} \alpha_1 = B_1a_{11} + B_2 \\ \alpha_2 = B_1a_{12} \\ \alpha_3 = B_1b_1 \end{cases} \tag{15}$$

The tracking error and its time derivative, respectively, are therefore given as:

$$e_\lambda = \alpha_1(\beta - \beta_d) + \alpha_2(\dot{\psi} - \dot{\psi}_d) \tag{16}$$

$$\dot{e}_\lambda = \alpha_1(\dot{\beta} - \dot{\beta}_d) + \alpha_2(\ddot{\psi} - \ddot{\psi}_d). \tag{17}$$

From the simplified model in (6), actual and desired yaw rates accelerations are expressed as:

$$\ddot{\psi} = a_{21}\beta + a_{22}\dot{\psi} + b_2\delta + b_3M_{z1} \tag{18}$$

$$\ddot{\psi}_d = a_{21}\beta_d + a_{22}\dot{\psi}_d + b_2\delta. \tag{19}$$

From time derivative of (7):

$$\dot{V}_1 = e_\lambda\dot{e}_\lambda. \tag{20}$$

From expressions (8) and (20):

$$\dot{e}_\lambda = \frac{-k_1}{2}e_\lambda. \tag{21}$$

Developing (17) gives:

$$\begin{aligned} \dot{e}_\lambda = \alpha_1(\dot{\beta} - \dot{\beta}_d) + \alpha_2(a_{21}(\beta - \beta_d) \\ +a_{22}(\dot{\psi} - \dot{\psi}_d) + b_3M_{z1}). \end{aligned} \tag{22}$$

By replacing (22) in (21), the continuous control input M_{z1} for lateral stability can be calculated as:

$$M_{z1} = \frac{1}{\alpha_2 b_3}[\mathcal{K}_1(\beta - \beta_d) + \mathcal{K}_2(\dot{\beta} - \dot{\beta}_d) + \mathcal{K}_3(\dot{\psi} - \dot{\psi}_d)], \tag{23}$$

where

$$\begin{cases} \mathcal{K}_1 = -\dfrac{k_1\alpha_1}{2} - \alpha_2a_{21} \\ \mathcal{K}_2 = -\alpha_1 \\ \mathcal{K}_3 = -\dfrac{k_1\alpha_2}{2} - \alpha_2a_{22}, \end{cases} \tag{24}$$

and k_1 is the controller's gain to be tuned. The particularity of this method is to not only control the side slip angle but also its derivative in such a way that the system's behavior is closer to the reference one.

3.4 Steerability control

The steerability controller attempts to force the vehicle to follow the reference yaw rate intended by the driver through driving the tracking error between the actual and desired yaw rate $e_{\dot{\psi}}$ to zero. It only matters when the system behaves in the linear driving region. In such driving situation, the stability controller is idle.
Following the same approach as for the stability controller design, the candidate Lyapunov function for steerability control is:

$$V_2 = \frac{1}{2}e_{\dot{\psi}}^2, V_2 > 0, V_2(0) = 0. \tag{25}$$

For an exponential stability:

$$\dot{V}_2 = -k_2V_2, \forall k_2 > 0. \tag{26}$$

It can be deduced that:

$$\dot{V}_2 = e_{\dot{\psi}}\dot{e}_{\dot{\psi}} = -\frac{k_2}{2}e_{\dot{\psi}}^2. \tag{27}$$

Therefore:

$$\ddot{\psi} - \ddot{\psi}_d = -\frac{k_2}{2}(\dot{\psi} - \dot{\psi}_d). \tag{28}$$

Based on expressions (18) and (19):

$$a_{21}(\beta - \beta_d) + a_{22}(\dot{\psi} - \dot{\psi}_d) + b_3M_{z2} = -\frac{k_2}{2}(\dot{\psi} - \dot{\psi}_d). \tag{29}$$

Finally, the continuous control law M_{z2} is:

$$M_{z2} = \frac{1}{b_3}((-\frac{k_2}{2} - a_{22})(\dot{\psi} - \dot{\psi}_d) - a_{21}(\beta - \beta_d)), \tag{30}$$

where k_2 is the controller's gain to be tuned.

Remarks:

- *The decay rates k_1 and k_2 of the two tracking errors e_λ and $e_{\dot{\psi}}$ give guideline for choosing the yaw motion controllers time responses.*
- *The dynamic errors of e_λ and $e_{\dot{\psi}}$ consistently approach stable point zero. They evolve independently, in the sense that only one controller is activated at a given instant to decouple steerability and stability objectives.*
- *The subsystem controllers coordination is ensured according to the rule given in Section 2. Thus, if $|\lambda| > 1$, $M_z = M_{z1}$, else, $M_z = M_{z2}$.*

3.5 Lower-level controller : Torque allocation algorithm

The torque allocation distribution algorithm is designed to obtain the motor drive or brake torque at each wheel to provide the vehicle's yaw moment imposed by the upper level controller. The target is to meet the overall motion control objectives by coordinating the in-wheel-motors while optimizing some performance metrics: i.e, energy consumption [Castro et al. (2013)], and dynamics stability [Gaspar et al. (2015); Zhai et al. (2016)]. This section presents a simple symmetry torques distribution strategy inspired from [Zou et al. (2007); Zhao et al. (2015)] to minimize the influence of the control input M_z on the longitudinal vehicle's velocity for a better riding comfort. To keep the longitudinal dynamic performances when the yaw moment upper controller works, equal torques are applied on the two wheels on the same axle but in opposite directions. In this distribution way, the resultant longitudinal driving force induced by the yaw moment controller is zero, and thus, longitudinal velocity won't be affected. The front and rear axle loads F_{zf} and F_{zr} can be expressed as:

$$F_{zf} = \frac{mgl_r - ma_xh}{l_f + l_r} \tag{31}$$

$$F_{zr} = \frac{mgl_f + ma_xh}{l_f + l_r}, \tag{32}$$

where h is the height of the center of gravity, and a_x is the vehicle's longitudinal acceleration. Thus, the load distribution ratio between front and rear axles is given by:

$$\kappa = \frac{mgl_r - ma_x h}{mgl_f + ma_x h} = \frac{F_{zf}}{F_{zr}}. \quad (33)$$

If the vehicle moves at a constant speed, than κ will be only function of the vehicle's geometry: $\kappa = \frac{l_r}{l_f}$. Otherwise, κ becomes a dynamic parameter depending on the vehicle's acceleration/deceleration.
Assuming small δ, the sum of the adjustment longitudinal forces ΔF_{ij} is given by:

$$\Delta F_{xfl} + \Delta F_{xfr} + \Delta F_{xrl} + \Delta F_{xrr} = 0, \quad (34)$$

where $i \in \{f = front, r = rear\}$, $j \in \{l = left, r = right\}$. The yaw moment M_z is realized with differential drive/brake torques of the in-wheel engine as follows:

$$M_z = (-\Delta F_{xfl} + \Delta F_{xfr} - \Delta F_{xrl} + \Delta F_{xrr})\frac{b}{2}, \quad (35)$$

where b is the vehicle's track. According to the load distribution between front and rear axles, it can be deduced that:

$$\frac{\Delta F_{xfl}}{\Delta F_{xrl}} = \kappa. \quad (36)$$

Rearranging equations (34),(35) and (36), the adjusted wheel forces can be written as:

$$\Delta F_{xfl} = -\frac{M_z}{b(1+\frac{1}{\kappa})}, \Delta F_{xrl} = \frac{1}{\kappa}\Delta F_{xfl} \quad (37)$$

$$\Delta F_{xfr} = +\frac{M_z}{b(1+\frac{1}{\kappa})}, \Delta F_{xrr} = \frac{1}{\kappa}\Delta F_{xfr}. \quad (38)$$

The adjustment torque to be generated by each in-wheel engine can be expressed as $\Delta T_{ij} = R_e \Delta F_{xij}$, where R_e is the tire's effective radius. This allocation method is suitable for real-time implementation, and does not involve any online optimization algorithm.

3.6 Electric motor model

The low-level current (voltage) control of the in-wheel-motor is not studied in this paper. Instead, a simplified first-order electric motor is applied to relate the torque command ΔT_{ij} defined by the lower controller at each wheel, and the effective motor torque ΔT^*_{ij} generated by the electric motor:

$$\Delta T^*_{ij} = \frac{\Delta T_{ij}}{1 + (L_m/R_m)s}, \quad (39)$$

where L_m and R_m are the motor's internal inductance and resistance, respectively.

4. SIMULATION RESULTS AND ANALYSIS

The developed control scheme is implemented in Matlab/Simulink environment. A nonlinear IWM-EV model is used to assess the closed loop performances. The nonlinear vehicle model includes: nonlinear tire behavior computed with a full Dugoff model, suspension dynamics, pitch and roll motions, and load transfers due to steering wheel and accelerations. The control approach was tested in different driving situations, however, due to lack of space, only one scenario is studied in the following. Responses of the passive vehicle (without control) and controlled vehicle are illustrated and compared.

4.1 Results

The simulated IWM-EV is driven at high speed 100 km/h negotiating an aggressive DLC (Double Lane Change) maneuver with a peak steering angle about 8°. The test is performed on a road with $\mu = 0.8$. The lateral vehicle dynamics is largely excited to evaluate the control scheme performances. The recorded lateral acceleration signal reaches a maximum value about $7m/s^2$. The sideslip dynamics is reported in $(\beta, \dot{\beta})$ phase plane illustrated in Figure 3. The upper and lower boundaries are equivalent to $|\lambda| = 1$. It is clear that the vehicle with the integrated control operates in the safety zone with $|\lambda| < 1$, while the passive vehicle enters the dangerous unsafe zone. Figures 4 and 5 report the vehicle yaw rate and the sideslip angle evolutions, respectively. Compared to the uncontrolled vehicle, the vehicle with control reduces the yaw rate and sideslip pick values. It is shown that improving stability is at the expense of vehicle's steerability. The generated corrective torques ΔT_{fl} and ΔT_{rl} are shown in Figure 6. According to Section 3.5, $\Delta T_{fr} = -\Delta T_{fl}$ and $\Delta T_{rr} = -\Delta T_{rl}$. The torques toggle from positive (drive) to negative (brake) values depending on the direction of the steering wheel angle, and on the signs of the tracking errors. The vehicle speed, after applying adjustment wheel torques, is almost equal to 97 km/h (velocity evolution figure is not shown here because of lack of space). This means that the longitudinal velocity is quasi-unchanged.

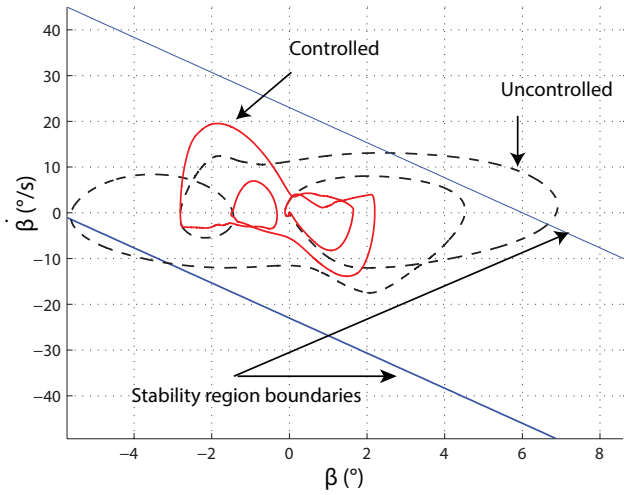

Fig. 3. Evolution of the controlled and uncontrolled vehicles in $(\beta, \dot{\beta})$ phase plane.

5. CONCLUSIONS

The focus of this paper is on presenting IWM-EVs lateral motion control in the framework of an advanced hierarchical multi-layer control strategy. The upper layer consists of two coordinated Lyapunov based controllers to improve EV dynamics behavior while avoiding conflicts between steerability and stability objectives. The coordination is ensured according to the vehicle running status and road friction information. Steerability target is prior when moving in linear zone, while stability is prior when the vehicle enters the unstable driving zone. The yaw moment generated by the upper control layer is converted by the lower layer into braking/driving torque at each wheel. A torque allocation method is proposed to effectively distribute the four wheel torques to achieve the control objectives with a minimum influence on the longitudinal vehicle speed. The benefit of the proposed method is that it could offer a concise and simple control procedure adequate for real-time implementation.

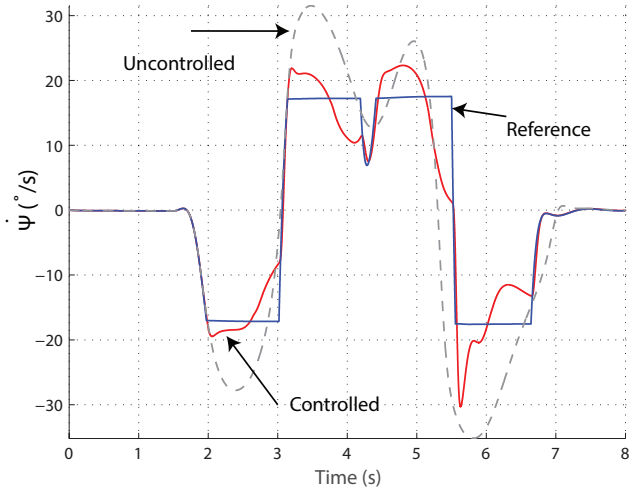

Fig. 4. Yaw rate responses of the controlled and uncontrolled vehicles.

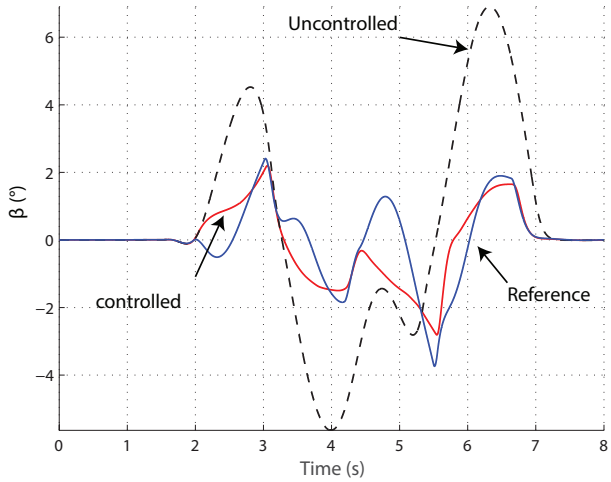

Fig. 5. Sideslip trajectories of the controlled and uncontrolled vehicles.

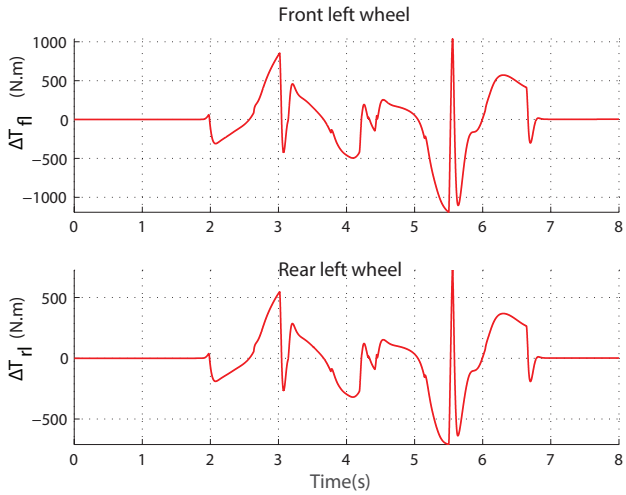

Fig. 6. Driving/braking torques applied by the controller to the left wheels.

Future work may consist to implement the proposed control strategy in an experimental IWM-EV. It is also crucial to study advanced and more sophisticated torque allocation methods to optimize EV energy consumptions under handling and dynamics stability constraints.

REFERENCES

M. Shino, and M. Nagai. Yaw moment control of electric vehicle for improving handling and stability. *Journal of Society of Automotive Engineers of Japan*, volume 22, pages 473-480, 2001.

J. He, D. Crolla, M.C. Levesley, and W.J. Manning. Integrated active steering and variable torque distribution control for improving vehicle handling and stability. *SAE World congress*, Detroit, USA, 2004.

G. Zou, Y. Luo, X. Lian, and K. Li. A research of DYC for independent 4WD EV based on control target dynamic regulated. *IEEE International Conference on Vehicular electronics and safety*, Beijing, China, 2007.

W. M. Haddad, and V. Chellaboina. Nonlinear dynamical systems and control. *Princeton University Press*, ISBN: 9780691133294, 2008.

R. Rajamani. Vehicle dynamics and control. *Springer US*, ISBN: 9781461414322, 2012.

M. Doumiati, A. Charara, A. Victorino, and D. Lechner. Vehicle Dynamics estimation using Kalman Filtering: Experimental validation. *J. Wiley-ISTE, Automation-Control and Industrial Engineering series*, ISBN: 978-1-84821-366-1, 2012.

K. Nam, H. Fujimoto, and Y. Hori. Lateral stability control of in-wheel-motor-driven electric vehicles based on sideslip angle estimation using lateral tire force sensors. *IEEE Transactions on Vehicular Technology*, volume 61, number 5, pages 1972-1985, 2012.

M. Doumiati, O. Sename, J. Martinez, L. Dugard, P. Gaspar, and Z. Szabo. Integrated vehicle dynamics control via coordination of active front steering and rear braking. *European Journal of Control*, volume 9, number 2, pages 923-941, 121-143, 2013.

Y. Chen, J.K. Hedrick, and K. Guo. A novel direct yaw moment controller for in-wheel motor electric vehicles. *Vehicle System Dynamics*, volume 51, number 6, pages 925-942, 2013.

R. Castro, M. Tanelli, R. Araújo, and S. Savaresi. Torque allocation in electric vehicles with in-wheel motors: a performance-oriented approach. *Proceedings of the 52nd IEEE Conference on Decision and Control*, Florence, Italy, 2013.

Z. Shuai, H. Zhang, J. Wang, J. Li, and M. Ouyang. Combined AFS and DYC control of four-wheel-independent-drive electric vehicles over CAN networks with time-varying delays. *IEEE Transactions on vehicular technology*, volume 63, number 2, pages 591-602, 2013.

M. Doumiati, A. Victorino, and A. Charara. Dynamics control of an in-wheel electric vehicle with steer-by-wire. *17th International Conference on Intelligent Transportation Systems (ITSC)*, Qingdao, China, 2014.

P. Gaspar, J. Bokor, A. Mihaly, Z. Szabo, T. Fulep, and F. Szauter. Robust reconfigurable control for in-wheel electric vehicles. *Proceedings of IFAC Symposium on Fault Detection, Supervision and Safety for Technical Processes*, Paris, France, 2015.

H. Zhao, BH. Gao, B. Ren, and H. Chen. Integrated control of in-wheel motor electric vehicles using a triple-step nonlinear method. *Journal of the Franklin Institute*, volume 352, pages 519-540, 2015.

L. Zhai, T. Sun, and J. Wang. Electronic stability control based on motor driving and braking torque distribution for a four in-wheel motor drive electric vehicle. *IEEE Transactions on Vehicular Technology*, volume 65, issue 6, pages 4726-4739, 2016.